PHYSICAL REVIEW A VOLUME 39, NUMBER 10 MAY 15, 1989

# Predictions of dendritic growth rates in the linearized solvability theory

A. Barbieri*
*Department of Physics, University of California, Santa Barbara, Santa Barbara, California 93106*

J. S. Langer
*Institute for Theoretical Physics, University of California, Santa Barbara, Santa Barbara, California 93106*
(Received 22 August 1988)

We obtain explicit predictions for velocity selection in two- and three-dimensional, symmetric, and one-sided models of dendritic solidification. We do this by using WKB techniques to derive a solvability condition, which is then solved numerically, for the existence of steady-state needle crystals. The comparison with available numerical results is reasonably good. We also discuss the comparison with experiments.

## I. INTRODUCTION

The solvability hypothesis seems currently to be the leading candidate for a first-principles theory of dendritic growth rates[1] and a number of other related phenomena as well. Our purpose in this paper is to present a relatively tractable form of this theory and its experimental predictions in a way that may lead to careful tests of its validity.

An elementary statement of the solvability hypothesis is the following. One attempts to model the tip of a growing dendrite by a needle crystal, that is, a shape-preserving steady-state growth form which is a solution of the equations of motion governing diffusion of heat or solute in the neighborhood of a solidification front. This needle crystal should be topologically similar to the parabolic solutions discovered by Ivantsov.[2] If capillary effects are included in specifying the boundary conditions on the front, then, according to the hypothesis, at most one dynamically stable solution will be found[3] for any given set of externally determined growth conditions, for example, for any fixed undercooling or supersaturation of the solidifying material. This unique needle crystal, if it exists, is supposed to be a stable attractor for the system. Its growth speed, the radius of curvature of its tip, and other properties such as the sensitivity to sidebranching deformations are supposed to be the same as those of experimentally observed dendrites[4–7] under the same conditions.

The solvability theory has achieved some notable theoretical successes, but its quantitative relevance to the interpretation of experimental data has not yet been established. The notion that the capillary effect is a singular perturbation which destroys Ivantsov's continuous family of solutions seems now to be confirmed by a wide variety of both analytic[8–11] and numerical studies.[12,13] Confirmation that the steady-state solution is actually an attractor for the fully dynamical system has been obtained in various local models of pattern formation and recently in a more realistic two-dimensional numerical simulation by Saito *et al.*[14] The solvability theory also explains why the stability parameter $\sigma^*$ (defined below) plays such a central role in dendritic pattern selection at small velocities. Finally, although the predicted dependence of $\sigma^*$ on the crystalline anisotropy has not so far been confirmed experimentally, it should be remembered that the solvability theory provides a very natural explanation for the fact that dendrites grow only in directions parallel to crystalline axes of symmetry; the lack of symmetry precludes the existence of solutions in other directions.

Uncertainties about the solvability theory stem principally from its apparent failure (by a factor of about 2—see below for a more detailed account) to predict the value of $\sigma^*$ for succinonitrile, by far the most carefully studied material and one which ought to be well within the range of validity of the theory. At the time this paper is being written, it seems possible that this discrepancy will be removed by a new measurement of the strength of the crystalline anisotropy. Our proper interest here, however, is in possible failures of the theory. It is still conceivable that the solvability hypothesis is completely wrong. The dynamic fixed point that we are finding, even if we are computing it correctly, might be irrelevant, and the true behavior of the system might be some oscillatory or even more complicated motion that would be invisible in our steady-state calculations. It seems to us more likely, however, that the solvability theory is basically correct for substances like succinonitrile and that, if there is a theoretical mistake at all, the problem is simply in our computational technique.

Attempts to translate the solvability hypothesis into practical schemes for predicting dendritic geometries and growth rates fall into two principal categories. The direct approach is to use a computer to search for solutions of the fully nonlinear and nonlocal free-boundary problem that is posed by the steady-state equations of motion for the solidification front. This approach has been carried out successfully by several different groups of investigators[13,12,15,16] and has provided both confirmation of mathematical conjectures and useful quantitative information. This approach becomes extremely difficult, however, for three-dimensional anisotropic crystals. The second, more analytic, class of tech-

 

niques introduces approximations which should be accurate when the actual shape of the needle crystal is not too far from the Ivantsov solution, that is, when the capillary correction measured by $\sigma^*$ is in some sense small. This is the approach that we shall discuss here.

Within the broad category of analytic approaches there are several levels of accuracy and sophistication. Clearly the most elegant and most nearly rigorous of these is the nonlinear analysis of Pomeau, Combescot, and coworkers[10,17] which is based on unpublished ideas of Kruskal and Segur. These authors use what might be described as a method of matched asymptotics in the complex plane to avoid performing an unsystematic linearization at the beginning of the calculation, and are thereby able to probe very deeply into the mathematical structure of the problem. Their method still relies on being able to use $\sigma^*$ as a small parameter, however, and thus their final formulas pertaining to pattern selection turn out to be identical to those obtained by the simpler procedure outlined below.

The method that we have advocated in the past,[11] and which we shall develop further here, is one in which the equation for the solidification front is linearized in the deviation from the Ivantsov solution at the very beginning of the calculation. The result of this procedure is an inhomogeneous linear equation for which it is, in principle, very easy to deduce a solvability condition. This condition is generally expressed in the form

$$\Lambda(\sigma,\alpha,p)=0 , \tag{1.1}$$

where $\sigma$ is the stability parameter, $\alpha$ is the strength of the crystalline anisotropy, $p$ is the Peclét number (a measure of the undercooling or supersaturation, i.e., the driving force), and $\Lambda$ is a function, to be defined below, which is conveniently approximated by WKB methods. Solutions of (1.1) determine $\sigma=\sigma^*$ as a function of $\alpha$ and $p$. In previous papers, we and other authors have studied the behavior of $\Lambda$ in the limit of asymptotically small $\alpha$ and have deduced the relationship $\sigma^* \propto \alpha^{7/4}$. This asymptotic analysis turns out to be unnecessarily restrictive, however, even within the framework of our small-$\sigma$ approximation. A principal point to be made in this paper is that numerical evaluation of $\Lambda$ allows us to compute $\sigma^*(\alpha,p)$ for values of $\alpha$ which are well beyond the range where the $\alpha^{7/4}$ law is valid, and that these values of $\sigma^*$ agree quite well with values computed by direct numerical solution of the original equations.

The organization of this paper is as follows. In Sec. II we consider the simplest possible case given by the two-dimensional symmetric model of solidification. Because almost all the numerical simulations have been performed on this model, this part will serve as an important test of the validity of the approximations employed. In Sec. III we show how to generalize the analysis to a three-dimensional model in which the effects of azimuthal anisotropy have been averaged out. Finally, in Sec. IV, we deal with the necessary modifications needed in the case in which the model is nonsymmetric, that is, when the relevant transport properties in the solid and in the liquid are different. This part includes as a special case the one-sided model and allows us to make a direct comparison with a recent experiment of Dougherty *et al.*[7] on ammonium bromide dendritic crystals.

## II. TWO-DIMENSIONAL SYMMETRIC MODEL OF SOLIDIFICATION

We start by writing down the dimensionless form of the equation of motion describing the solidification of a pure substance in the general nonsymmetric case. In this paper we will use the terminology and notation pertaining to thermally driven solidification, but the same model applies to the case in which the mechanism of growth is instead given by the diffusion of one chemical species away from the solidifying interface.[18] The equations are

$$\nabla^2 u_i = 2p_i \frac{\partial \mu_i}{\partial t}, \quad i=L,S \tag{2.1}$$

$$2p_L v_n = \mathbf{n}\cdot(\mu \nabla u_S|_{\text{front}} - \nabla u_L|_{\text{front}}) , \tag{2.2}$$

$$u|_{\text{front}} = \Delta - \frac{d_0}{\rho}\mathcal{K}, \quad u_L|_{\text{front}} = u_S|_{\text{front}} . \tag{2.3}$$

$L$ and $S$ refer to the liquid and solid, respectively, and $u_i=(T_i-T_\infty)c_L/L$ is the appropriately rescaled temperature field in the $i$th phase, measured from the temperature at infinity $T_\infty$. The material properties defining the dimensionless parameters in (2.1)–(2.3) are the specific heat $c_i$, the latent heat of solidification per unit volume $L$, the thermal diffusion constant $D_i$, the bulk melting temperature of the substance $T_M$, and the surface tension $\gamma$ which will be allowed to include the effect of crystalline anisotropy in a way to be specified later. In terms of these parameters, $\Delta=(T_M-T_\infty)c_L/L$ is the dimensionless undercooling, $\mu=D_S c_S/D_L c_L$ is a measure of the asymmetry of the two phases, and $d_0=\gamma T_M c_L/L^2$ is a capillary length proportional to the surface tension; $\rho$ is an appropriate unit of length which will be identified later on with the tip radius of curvature of the Ivantsov solution moving with velocity $v$ and, finally, $p_i=\rho v/2D_i$ is the Peclét number.

The physics underlying Eqs. (2.1)–(2.3) is quite simple. A moving, solidifying front releases latent heat which diffuses to infinity as expressed by (2.1); requiring heat conservation at the interface gives us (2.2) ($\mathbf{n}$ is the normal to the front pointing into the liquid and $v_n$ is the normal velocity of the front), while imposing local thermodynamic equilibrium in the interfacial region implies (2.3). Equation (2.3) is the well-known Gibbs-Thomson relation, which gives the equilibrium value of the temperature at the interface and takes into account curvature corrections; we will be more specific about the precise form of this curvature term as we go along with the analysis.

An equivalent formulation of the problem which is more convenient for our purposes is obtained by eliminating the thermal field from the equations; this can be done by using standard Green's function techniques[9] to obtain an equation in closed form for the function describing the solid-liquid interface. In the two-dimensional symmetric

model ($\mu=1, p_L=p_S$) the equation reads

$$\Delta+\frac{\bar{d}_0}{\rho}A(\zeta')\frac{\zeta''(x)}{(1+\zeta'^2)^{3/2}}=p\int_{-\infty}^{+\infty}\frac{dx'}{\pi}e^{-p[\zeta(x)-\zeta(x')]}\times K_0(p\eta(x,x'))\ , \tag{2.4}$$

where

$$\eta(x,x')=\{(x-x')^2+[\zeta(x)-\zeta(x')]^2\}^{1/2}\ , \tag{2.5}$$

$(x,\zeta(x))$ represent the Cartesian coordinates of the solidification front in a moving frame in which the front is at rest, $K_0$ is the Bessel function of the third kind of order zero,[19] and prime superscripts denote derivatives with respect to $x$. The right-hand side of (2.4) is equal to the temperature of the interface at the point $(x,\zeta(x))$ as computed by using (2.1)–(2.2); the left-hand side is the same temperature obtained by imposing the Gibbs-Thomson relation (2.3).

The function $A(\zeta')$ describes the dependence of the capillary length $d_0$ on the orientation of the interface relative to the crystalline axes. In two dimensions we have $d_0=\bar{d}_0 A(\zeta')$ and, to be specific, we assume the usual fourfold symmetric form $A(\theta)=1-\alpha\cos 4\theta$, $\theta$ being the angle between the normal to the front and the $z$ direction, and $\alpha$ the anisotropy strength. Since $\zeta'=-\tan\theta$ we have

$$A(\zeta')=1-\alpha+\frac{8\alpha\zeta'^2}{(1+\zeta'^2)^2}\ . \tag{2.6}$$

It is well known that a solution of (2.4) when $\bar{d}_0=0$ is given by

$$\zeta_{iv}(x)=-\frac{x^2}{2}\ ,$$

$$\Delta=2\sqrt{p}\,e^p\int_{\sqrt{p}}^{\infty}dy\,e^{-y^2}\ , \tag{2.7}$$

where the length scale $\rho$ has been chosen to be equal to the radius of curvature of the tip. Note that $\rho$ is the tip radius of the Ivantsov ($\bar{d}_0=0$) parabola with undercooling $\Delta$, moving at speed $v$. Equation (2.7) corresponds to the famous Ivantsov continuous family solutions,[2] and we will be interested in solutions of (2.4) which are asymptotic to an Ivantsov parabola as $x\to\pm\infty$.

Following Pelcé *et al.*[8] we now replace $\Delta$ on the left-hand side of (2.4) with its integral representation in terms of $\zeta_{iv}(x)$; we obtain in this way

$$\sigma A[\zeta'(x)]\frac{\zeta''}{(1+\zeta'^2)^{3/2}}=\int_{-\infty}^{+\infty}\frac{dx'}{\pi}[e^{-p[\zeta(x)-\zeta(x')]}K_0(p\{(x-x')^2+[\zeta(x)-\zeta(x')]^2\}^{1/2})-(\zeta\leftrightarrow\zeta_{iv})]\ , \tag{2.8}$$

where $\sigma=\bar{d}_0/p\rho(v,\Delta)=\bar{d}_0 v/2Dp^2$. The problem we have to solve now is essentially a nonlinear eigenvalue problem: Given $p$ [which, through (2.7), is related to a particular value of the undercooling] we want to determine the values of $\sigma$ such that (2.8) admits smooth solutions which tend to an Ivantsov parabola as $x\to\pm\infty$.

The analysis will now follow that of Ref. 11 with the exception of two important points. The first is that there is no need, as explained by Caroli *et al.*,[20] to take the limit $p\to 0$ in (2.8). We will see that it is possible in this way to obtain finite-$p$ corrections to the selected value of $\sigma$. The second difference is that we do not at the beginning assume $\alpha$ to be small, and this will turn out to be important to obtain an accurate estimate of $\sigma^*$. As in Ref. 11, we will analyze Eq. (2.8) in the limit $\sigma\ll 1$ and, at the end of the calculation, we will check that the selected value $\sigma^*$ does indeed play the role of a small parameter.

As a first step we substitute $\zeta=\zeta_{iv}+\zeta_1$ in (2.8), and linearize in $\zeta_1$. This linearization (note that this is not a linearization in the small parameter $\sigma$) is not mathematically very well controlled and, as we mentioned in the Introduction, could be avoided[10] by performing a matched asymptotic analysis in the complex $x$ plane. We will see, however, that the linearization seems to give the correct asymptotic form of $\sigma^*(\alpha)$ anyway[21] and, being easier to implement, can be applied in a straightforward way to more complicated situations.[22] The result of the linearization is the following equation for $\zeta_1$:

$$\sigma Af=\sigma\frac{d}{dx}(Af\zeta_1')+p\int_{-\infty}^{+\infty}\frac{dx'}{\pi}[\zeta_1(x)-\zeta_1(x')]e^{-(p/2)(x'^2-x^2)}\left[K_0(p\eta_{iv})+\frac{(x'^2-x^2)}{2\eta_{iv}(x,x')}K_1(p\eta_{iv})\right]\ , \tag{2.9}$$

where

$$f(x)=\frac{1}{(1+x^2)^{3/2}},\quad A(x)=1-\alpha+\frac{8\alpha x^2}{(1+x^2)^2}\ , \tag{2.10}$$

and, following the notation of (2.5),

$$\eta_{iv}(x,x')=[(x-x')^2+\tfrac{1}{4}(x'^2-x^2)^2]^{1/2}\ .$$

We can now split the integral in (2.9) using a principal part regularization, evaluate[20] the integral multiplying $\zeta_1(x)$, and change variable to

$$Z(x)=\sqrt{Af}\,\zeta_1(x)\ . \tag{2.11}$$

Being interested in the limit $\sigma\to 0$ we can neglect terms of order $\sigma Z(x)$ and obtain

$$\sigma Z''(x)+\frac{(1+x^2)^{1/2}}{A(x)}Z(x)-p\mathcal{P}\int_{-\infty}^{+\infty}\frac{dx'}{\pi}Z(x')I(x,x')=\sigma\frac{\sqrt{A(x)}}{(1+x^2)^{3/4}}\ , \tag{2.12}$$

where the nonsymmetric kernel $I(x,x')$ is given by

$$I(x,x')=e^{-(p/2)(x'^2-x^2)}\frac{[(1+x^2)(1+x'^2)]^{3/4}}{\sqrt{A(x)A(x')}}\left[K_0(p\eta_{iv})+\frac{1}{2}\frac{(x'^2-x^2)}{\eta_{iv}}K_1(p\eta_{iv})\right]\ . \tag{2.13}$$

Equation (2.12) is of the form $\mathcal{L}Z=g$, where $\mathcal{L}$ is a linear operator and $g$ is the inhomogeneous term appearing in (2.12); this structure suggests by itself the solvability condition that we have to impose. If we find a nontrivial null eigenvector of the adjoining operator $\mathcal{L}^\dagger$, i.e., a solution of the equation $\mathcal{L}^\dagger\tilde{Z}=0$, then we immediately have a necessary condition for the existence of solutions of (2.12). Indeed we have

$$\Lambda\equiv(\tilde{Z},g)=(\tilde{Z},\mathcal{L}Z)=(\mathcal{L}^\dagger\tilde{Z},Z)=0\ , \tag{2.14}$$

where $(\cdot,\cdot)$ denotes the inner product related to the definition of the adjoint operator; in words, the kernel of the adjoint operator must be orthogonal to the inhomogeneous term appearing in (2.12). It is worth mentioning that the direct operator $\mathcal{L}$ has an obvious null eigenvector, namely, any constant function is a solution of $\mathcal{L}Z=0$ as we can immediately verify by considering Eq. (2.9). This is the natural manifestation of the translational invariance of the system along the $z$ direction. For this reason we can expect, in principle, that also the adjoint operator has a null eigenvector which makes the solvability condition (2.14) nontrivial.[23]

The main advantage of the solvability approach is that we have to solve a homogeneous, rather than inhomogeneous, equation. If we define the inner product in the usual way as $(f,g)=\int_{-\infty}^{+\infty}dx\,f^*(x)g(x)$, the differential part of $\mathcal{L}$ becomes self-adjoint and the equation $\mathcal{L}^\dagger\tilde{Z}=0$ can be written as

$$\sigma\tilde{Z}''(x)+\frac{(1+x^2)^{1/2}}{A(x)}\tilde{Z}(x)-p\mathcal{P}\int_{-\infty}^{+\infty}\frac{dx'}{\pi}\tilde{Z}(x')I(x',x)=0\ . \tag{2.15}$$

In order to solve this equation we assume a WKB form for $\tilde{Z}(x)$, i.e., we make the ansatz

$$\tilde{Z}(x)=\exp\left[\frac{S(x,\sigma)}{\sqrt{\sigma}}\right]\ , \tag{2.16}$$

where

$$S(x,\sigma)=\sum_{n=0}^{\infty}\sigma^{n/2}S_n(x)\ . \tag{2.17}$$

This ansatz is particularly useful in solving Eq. (2.15) because it allows us to replace the integral term with a local one and then to obtain an explicit solution of the equation in the limit $\sigma\to0$. The details of the calculation are reported in Appendix A.

It turns out that Eq. (2.15) admits a complex-conjugate pair of solutions $\tilde{Z}(x)$ and $\tilde{Z}^*(x)$ whose form, correct up to the term $S_1$ in (2.17), is given by

$$\tilde{Z}(x)=\frac{A^{1/4}}{(1+x^2)^{3/8}}(1-ix)^{1/4}\times\exp\left[\frac{S_0(x)}{\sqrt{\sigma}}-\frac{p}{2}\left[ix+\frac{x^2}{2}\right]\right]\ , \tag{2.18}$$

where

$$S_0(x)=i\int_0^x dx'\frac{(1-ix')^{1/4}(1+ix')^{3/4}}{A^{1/2}(x')}\ . \tag{2.19}$$

The function $\tilde{Z}(x)$ is well behaved at $\infty$ and satisfies $\tilde{Z}(-x)=\tilde{Z}^*(x)$; the solvability condition (2.14) for the existence of well-behaved, even solutions of (2.12) can therefore be written explicitly in the form

$$\Lambda_2(\sigma,\alpha,p)=\int_{-\infty}^{+\infty}dx'\tfrac{1}{2}[\tilde{Z}(x')+\tilde{Z}(-x')]\frac{A^{1/2}}{(1+x'^2)^{3/4}}=\int_{-\infty}^{+\infty}dx'\frac{\tilde{Z}(x')A^{1/2}}{(1+x'^2)^{3/4}}=0\ , \tag{2.20}$$

where the solvability function $\Lambda(\sigma,\alpha,p)$ is real due to the symmetry properties of $\tilde{Z}(x)$.

It can be shown that for any fixed value of $\alpha$ the function $\Lambda_2(\sigma,\alpha,p)$ has a denumerable set of zeros $\sigma_n(\alpha,p)$ accumulating towards $\sigma=0$ as $n\to\infty$. We could obtain an analytic expression for $\sigma_n(\alpha,p)$ in the limit $n\to\infty$ but we are actually interested in the maximum allowed value of $\sigma$ which is customarily denoted by $\sigma^*$ and is believed to correspond to the only linearly stable needle crystal.[8] This value is best obtained by a direct numerical solution of (2.20) which is plotted in Fig. 1 for the two values $p=0$ and $p=0.25$; the comparison with the available numerical results[15,12] is reasonably good even for relatively high values of the anisotropy strength $\alpha$. Of course, the entire approximation scheme is expected to break down for $\alpha$ large enough that $\sigma^*$ is no longer small. Our comparison with the direct numerical results indicates that our method remains reasonably accurate for values of $\alpha$ up to 0.5 or 0.6.[24] Notice that the expected asymptotic behavior,[11] $\sigma^*\propto\alpha^{7/4}$ when $\alpha\to0$, sets in only for very small values of $\alpha$, typically $\alpha<0.01$.

## III. THREE-DIMENSIONAL SYMMETRIC MODEL

The corresponding analysis in the three-dimensional case is more difficult but conceptually very similar to that presented in Sec. II. The first complication arises when, in order to understand what we mean by $d_0\mathcal{H}$ in (2.3), we want to generalize the Gibbs-Thomson relation to the case of cubic anisotropy.

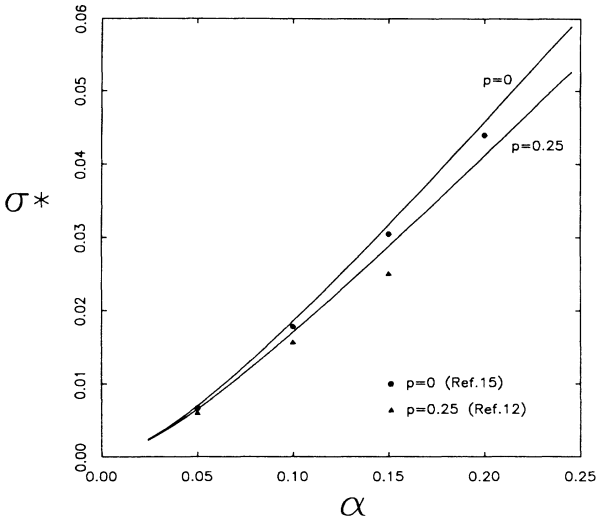


FIG. 1. Selected values $\sigma^*$ as a function of the anisotropy strength $\alpha$ for $p=0$ and $p=0.25$ in two dimensions. Comparison with a direct numerical integration of Eq. (2.4).

It is well known[25] that the Gibbs-Thomson relation in the three-dimensional case with anisotropic surface energy is given by

$$T-T_M=-\frac{T_M}{L}\left[\frac{1}{R_1}\left[\gamma+\frac{\partial^2\gamma}{\partial\theta_1^2}\right]+\frac{1}{R_2}\left[\gamma+\frac{\partial^2\gamma}{\partial\theta_2^2}\right]\right], \tag{3.1}$$

where $R_1$, $R_2$ are the local principal radii of curvature of the surface, $\theta_1,\theta_2$ are the angles between the normal $\mathbf{n}$ and the local principal directions on the surface, and $\gamma(\mathbf{n})$ is the anisotropic surface energy. For the purpose of both numerical and analytical computation, it would be more convenient to express $\partial^2\gamma/\partial\theta_i^2$ directly in terms of the variation of $\gamma$ with respect to the two angles defining the direction of the normal with respect to a fixed set of crystal axes. Unfortunately, because the definition of $\theta_1$ and $\theta_2$ involves the principal directions on the interface, the corresponding expression one obtains is quite complicated[16] and the problem becomes analytically too difficult for present purposes.

In order to simplify the analysis we will make two assumptions. First we assume that solutions exist only when the crystal is growing along an axis of symmetry; although this fact has not been proved rigorously, it is strongly suggested by the mathematical structure of the solvability theory. The second, more important, and potentially more dangerous, assumption is that $\gamma$ in (3.1) depends only on the polar angle $\tilde{\theta}$ between $\mathbf{n}$ and the fixed direction in space corresponding to the axis of growth. This allows us to consider axisymmetric solutions and to replace (3.1) with

$$T-T_M=-\frac{T_M}{L}\left[\frac{1}{R_1}\left[\gamma+\frac{\partial^2\gamma}{\partial\tilde{\theta}^2}\right]+\frac{1}{R_2}\left[\gamma+\cot\tilde{\theta}\frac{\partial\gamma}{\partial\tilde{\theta}}\right]\right], \tag{3.2}$$

which can be derived from (3.1) by simple geometrical considerations. The only check we have on this approximation comes from the numerical results reported in the literature[16] which suggest that indeed azimuthal anisotropy does not play an important role in the steady-state selection mechanism. The main reason for us to adopt such a point of view is that it greatly simplifies the analysis and it makes it possible to obtain, in a relatively simple way, explicit predictions for the value of $\sigma^*$ even in the three-dimensional case.

We now discuss briefly the appropriate form to use for $\gamma(\tilde{\theta})$ in (3.2). The simplest possible function describing the dependence of surface energy on $\mathbf{n}$ in the case of an underlying cubic symmetry can be written as

$$\gamma(\mathbf{n})=\bar{\gamma}'[1+\epsilon'(n_x^4+n_y^4+n_z^4)]$$
$$=\bar{\gamma}'\{1+\epsilon'[\cos^4\tilde{\theta}+\sin^4\tilde{\theta}(1-2\sin^2\tilde{\phi}\cos^2\tilde{\phi})]\}, \tag{3.3}$$

where $\tilde{\theta}$ and $\tilde{\phi}$ are the spherical angles which define $\mathbf{n}$ with respect to a crystal axis. The parameter $\epsilon'$ in (3.3) can be related to the definition of anisotropy strength appearing in the experimental literature[5,7] in the following way. Usually, the anisotropy strength is computed by measuring the deviation from spherical shape of a single crystal close to equilibrium. In particular, if the form of $\gamma(\mathbf{n})$ in the (100) plane is given by

$$\gamma=\bar{\gamma}(1+\epsilon_4\cos4\tilde{\theta}+\cdots), \tag{3.4}$$

the angular dependence of the radius of the crystal in the same plane is[26]

$$R(\tilde{\theta})=R_0(1+\epsilon_4\cos4\tilde{\theta}+\cdots).$$

By considering (3.3) when $\tilde{\phi}=0$, and comparing with (3.4) we obtain that $\epsilon_4=\epsilon'/(4+3\epsilon')$. As mentioned already, however, we want to consider an axisymmetric version of (3.3) which allows us to consider axisymmetric needle-crystal solutions. For this purpose, we average (3.3) over $\tilde{\phi}$ and replace this equation with

$$\gamma(\mathbf{n})=\bar{\gamma}'[1+\epsilon'(\cos^4\tilde{\theta}+\tfrac{3}{4}\sin^4\tilde{\theta})]$$
$$=\bar{\gamma}\left[1+\frac{\alpha}{15}\cos4\tilde{\theta}-\frac{\alpha}{15}\sin^4\tilde{\theta}\right], \tag{3.5}$$

where the relation between $\alpha$ and $\epsilon_4$ is easily determined to be

$$\frac{\alpha}{15}=\epsilon_4.$$

The factor of 15 has been inserted because of the similarity between (3.5) and the analogous two-dimensional expression.

We can now proceed with the analysis of the equation

of motion. Within the approximations just described, the Gibbs-Thomson correction in (2.3) is determined by the term in square brackets on the right-hand side of (3.2) and the three-dimensional equation analogous to (2.4) reads

$$\Delta-\frac{\bar{d}_0}{\rho}\left[\frac{A(\tilde{\theta})}{R_1}+\frac{B(\tilde{\theta})}{R_2}\right] =p\int\frac{d\mathbf{x}'}{2\pi}\frac{\exp\{p[\zeta(r')-\zeta(r)]-p\eta(\mathbf{x},\mathbf{x}')\}}{\eta(\mathbf{x},\mathbf{x}')}\ , \tag{3.6}$$

where

$$\frac{1}{R_1}=-\frac{d}{dr}\left[\frac{\zeta'}{(1+\zeta'^2)^{1/2}}\right],\quad \frac{1}{R_2}=-\frac{\zeta'}{r(1+\zeta'^2)^{1/2}}\ , \tag{3.7}$$

$$\bar{\gamma}A(\tilde{\theta})=\gamma+\frac{\partial^2\gamma}{\partial\tilde{\theta}^2},\quad \bar{\gamma}B(\tilde{\theta})=\gamma+\cot\tilde{\theta}\frac{\partial\gamma}{\partial\tilde{\theta}}\ , \tag{3.8}$$

with $\gamma(\tilde{\theta})$ given by (3.5) and $\tan\tilde{\theta}=-\zeta'(r)$. Here and in the following $\mathbf{x}$ is a two-dimensional vector whose modulus is denoted by $r$ while $\eta(\mathbf{x},\mathbf{x}')$ represents, as in two dimensions, the Euclidean distance between the corresponding points on the solidification front.

The strategy is now identical to the one used in Sec. II. We make use of the three-dimensional Ivantsov solution

$$\zeta_{iv}(r)=-\frac{r^2}{2}\ ,\qquad \Delta=pe^p\int_p^\infty dy\frac{e^{-y}}{y}\ , \tag{3.9}$$

and linearize (3.6) in order to obtain the desired solvability condition. When we do this an important simplification, described in Appendix B, allows us to write the linearized version of (3.6) in the following compact form which is the three-dimensional analog of (2.9):

$$\frac{\sigma}{r}\frac{d}{dr}[rAf\zeta_1']+\int\frac{d\mathbf{x}'}{2\pi}\exp\left[-\frac{p}{2}(r'^2-r^2)-p\eta_{iv}\right]\left[\frac{p}{\eta_{iv}}+\frac{r'^2-r^2}{2\eta_{iv}^2}\left[p+\frac{1}{\eta_{iv}}\right]\right][\zeta_1(r)-\zeta_1(r')]=\sigma\mathcal{H}_{iv}\ ; \tag{3.10}$$

$\mathcal{H}_{iv}$, $f$, and $A$ are given by (B1), (B2), and (B3), respectively. Once again we can compute the integral multiplying $\zeta_1(r)$, change variable to $Z(r)=\sqrt{rfA}\,\zeta_1(r)$, and finally obtain

$$\sigma Z''(r)+\left[\frac{\sigma}{4r^2}+\frac{(1+r^2)}{A(r)}\right]Z(r)-p\mathcal{P}\int_0^\infty\frac{dr'}{\pi}Z(r')H(r,r')=\sigma\frac{\sqrt{r}\,(1+r^2)^{3/4}}{\sqrt{A}}\mathcal{H}_{iv}\ . \tag{3.11}$$

The integral kernel is now given by

$$H(r,r')=\frac{(1+r^2)^{3/4}(1+r'^2)^{3/4}}{2\sqrt{A(r)A(r')}}\sqrt{rr'}\int_0^{2\pi}d\phi\exp\left[-\frac{p}{2}(r'^2-r^2)-p\eta_{iv}(r,r',\phi)\right]\left[\frac{1}{\eta_{iv}}+\frac{r'^2-r^2}{2\eta_{iv}^2}\left[1+\frac{1}{p\eta_{iv}}\right]\right]\ , \tag{3.12}$$

where $\phi$ is the angle between $\mathbf{r}$ and $\mathbf{r}'$ and hence

$$\eta_{iv}=[r^2+r'^2-2rr'\cos\phi+\tfrac{1}{4}(r'^2-r^2)^2]^{1/2}\ .$$

In writing (3.11) we have neglected a term of order $\sigma\tilde{f}(r)Z(r)$, with $\tilde{f}(r)$ smooth and regular at the origin; the term $\sigma Z(r)/4r^2$, however, must be kept because it becomes important when $r$ is sufficiently close to the origin ($r<\sqrt{\sigma}$).

The last thing we need to specify in order to write down the solvability condition in three dimensions is the boundary condition to impose on $Z$ at $r=0$. Note that, in this case, functions are defined for $r\geq 0$ only, and the inner product in (2.14) implies an integration on this restricted domain. In other words we have to characterize the function space on which the operator $\mathcal{L}$ acts so that (2.14) is valid.

If we consider the relation between $Z$ and $\zeta_1$, and the physical meaning of $\zeta_1(r)$, it should be clear that we are interested in solutions of (3.11) which go to zero at least as fast as $\sqrt{r}$ when $r\to 0$. One can check that (2.14) is still the correct solvability condition with $\tilde{Z}(r)$ defined by the equation $\mathcal{L}^\dagger\tilde{Z}=0$

$$\sigma\tilde{Z}''(r)+\left[\frac{\sigma}{4r^2}+\frac{(1+r^2)^{1/2}}{A(r)}\right]\tilde{Z}(r) -p\mathcal{P}\int_0^\infty\frac{dr'}{\pi}\tilde{Z}(r')H(r',r)=0\ , \tag{3.13}$$

supplemented by the boundary condition $\tilde{Z}(r)\propto\sqrt{r}$ as $r\to 0$. This homogeneous equation for $\tilde{Z}(r)$ is the analog of the two-dimensional equation (2.15) and we can obtain an approximate solution for small $\sigma$ in a way similar to the one employed in the previous case. (See Appendix B.)

The appropriate solution of (3.13) satisfying the boundary condition at the origin is

$$\tilde{W}(r)=e^{-i(\pi/4)}\tilde{Z}(r)+e^{+i(\pi/4)}\tilde{Z}^*(r)\ , \tag{3.14}$$

where $\tilde{Z}(r)$ is again given by (2.18) and (2.19) provided we use (B3) for $A(r)$. This is the null eigenvector of $\mathcal{L}^\dagger$ which must be used when computing the solvability condition, which now explicitly reads

$$\Lambda_3(\sigma,\alpha,p)=\int_0^\infty dr\,\tilde{W}(r)\frac{\sqrt{r}\,(1+r^2)^{3/4}}{\sqrt{A}}\mathcal{H}_{iv}$$

$$=\mathrm{Re}\int_0^\infty dr\frac{\sqrt{rA}}{(1+r^2)^{3/4}}\left[1+(1+r^2)\frac{B(r)}{A(r)}\right]\tilde{Z}(r)e^{-i(\pi/4)}=0\ , \tag{3.15}$$

with $A$ and $B$ given in Appendix B.

Note that, although the integration in (3.15) is for positive $r$ only, the resulting expression for $\Lambda_3(\sigma,\alpha,p)$ is very similar to what we found for $\Lambda_2(\sigma,\alpha,p)$. To see this we have to deform the contour of integration into the complex $r$ plane and notice that $\Lambda_3$ is dominated by the behavior of the integrand in a neighborhood of $r=i$, where the solvability integral has the same structure as in the two-dimensional case; for this reason one can expect to obtain similar results for $\Lambda_2$ and $\Lambda_3$.

Figure 2 shows $\sigma^*(\alpha)$ as obtained by a numerical solution of (3.15) for two different values of $p$; the two dots correspond to the numerical simulation of Ref. 16 which is the only one available, to our knowledge, in the case of a three-dimensional anisotropic system. Notice that the prediction of $\sigma^*$ is quite sensitive to the value of the anisotropy strength which, for this reason, should be measured with particular case. The comparison with the experimental data available in the case of succinonitrile,[5] a material which should be correctly described by the symmetric model of solidification, can be obtained by using the reported experimental value of $\alpha_{\mathrm{ex}}\simeq 0.075$. From (3.15) we get $\sigma^*\simeq 0.0092$ while experimentally $\sigma^*_{\mathrm{ex}}\simeq 0.0195$.

In the case of dendritic growth from a supersaturated ammonium bromide solution[7] the theory seems to be in better shape. This case actually corresponds to the one-sided rather than the symmetric limit [$\mu=0$ in Eqs. (2.1)–(2.3)] and we anticipate here the results derived in Sec. IV. Equation (4.3) gives us the necessary modification which allows us to compute $\sigma^*$. We have[7] $\alpha_{\mathrm{ex}}=0.24\pm 0.06$ and $\sigma^*_{\mathrm{ex}}=0.081\pm 0.02$ while the theory gives us $\sigma^*=0.083\pm 0.025$. The uncertainty about the predicted value of $\sigma^*$ comes from the reported uncertainty of $\alpha_{\mathrm{ex}}$ and does not include the error related to the approximations used to derive (3.15) and (4.3).

## IV. NONSYMMETRIC CASE

Finally, let us consider the more general nonsymmetric case. We will see that the value of $\sigma^*$ can be simply related to the analogous symmetric result just derived. We start by going back to Eqs. (2.1)–(2.3) and noticing that, for general values of $p$ and $\mu$, we can write down[22] an equivalent set of two integrodifferential equations for $\zeta(\mathbf{x})$ and, for example, the value of the normal component of the heat flux into the liquid,

$$-\int_S da'\left[\frac{d_0}{\rho}(\mathbf{n}\cdot\nabla'\mathcal{G}_L)\mathcal{H}+\mathcal{G}_L(\mathbf{n}\cdot\nabla' u_L)\right]+2p_L\frac{d_0}{\rho}\int d\mathbf{x}'\mathcal{G}_L\mathcal{H}=\Delta-\frac{d_0}{2\rho}\mathcal{H}\ , \tag{4.1a}$$

$$-\int_S da'\left[\mu\frac{d_0}{\rho}(\mathbf{n}\cdot\nabla'\mathcal{G}_S)\mathcal{H}+\mathcal{G}_S(\mathbf{n}\cdot\nabla' u_L)\right]+2p_S\mu\int d\mathbf{x}'\mathcal{G}_S\left[\frac{d_0}{\rho}\mathcal{H}-\frac{p_L}{p_S\mu}\right]=\frac{\mu}{2}\frac{d_0}{\rho}\mathcal{H}\ . \tag{4.1b}$$

In writing (4.1) we have again restricted attention to steady-state solutions moving with constant velocity $v$, $\int_S da'$ denotes an integration over the solidification front, and $\mathcal{G}_{L(S)}$ is the Green's function for steady-state diffusion in the appropriate moving frame

$$\mathcal{G}_i(\mathbf{r},\mathbf{r}')=\frac{1}{4\pi}\frac{\exp[p_i(z'-z)-p_i|\mathbf{r}-\mathbf{r}'|]}{|\mathbf{r}-\mathbf{r}'|}\ .$$

As in Sec. III, we consider only longitudinal anisotropy so that $\mathcal{H}$ is again given by the term in square brackets in (3.2).

Two things should be noticed about (4.1). The first is that if $\mu=1$ and $p_L=p_S$, then $\mathcal{G}_L=\mathcal{G}_S$ and, by subtracting (4.1b) from (4.1a), we recover, as we should, Eq. (3.6). The second is that, in the Ivantsov limit $d_0=0$, Eq. (4.1b) can be solved if we take $\mathbf{n}\cdot\nabla u_L=-2V_n p_L$, whereas Eq. (4.1a) reduces to the $d_0=0$ limit of Eq. (3.6). This simply reflects the fact that, without surface tension, we can always take the solid to be isothermal, in this way eliminating from the problem any reference to diffusion in the solid phase.

In order to make further analytic progress with (4.1), we now consider the physically relevant limit of small undercooling. Although it is very likely that the analysis could be generalized to arbitrary values of $p$ in a way analogous to what was done in the symmetric case,[27] we consider here the limit $\Delta\to 0$ for the sake of simplicity; indeed, in this limit Eqs. (4.1a) and (4.1b) can be reduced to a single equation which can be analyzed by using techniques we are already familiar with. To do this we first replace $\Delta$ in Eqs. (4.1a) and (4.1b) with its integral representation in terms of $\mathcal{G}_L(\mathbf{x}-\mathbf{x}',\zeta_{iv}(x)-\zeta_{iv}(x'))$, and then take the limit $p\to 0$. In this way Eqs. (4.1a) and (4.1b) can be combined in the form

$$\sigma(1-\mu)\int\frac{d\mathbf{x}'}{4\pi}\mathcal{K}[\zeta(\mathbf{x}')]\frac{\zeta(\mathbf{x}')-\zeta(\mathbf{x})-(\mathbf{x}'-\mathbf{x})\cdot\nabla'\zeta(\mathbf{x}')}{\{(\mathbf{x}-\mathbf{x}')^2+[\zeta(\mathbf{x})-\zeta(\mathbf{x}')]^2\}^{3/2}}+2\int\frac{d\mathbf{x}'}{4\pi}\left[\frac{1}{\sqrt{(\mathbf{x}-\mathbf{x}')^2+[\zeta(\mathbf{x})-\zeta(\mathbf{x}')]^2}}-(\zeta\leftrightarrow\zeta_{iv})\right]$$
$$=-\frac{\sigma}{2}(1+\mu)\mathcal{K}\ , \quad (4.2)$$

where, as usual, $\sigma=\bar{d}_0/\rho p_L$ and $\zeta_{iv}$ denotes the Ivantsov solution $\zeta_{iv}(\mathbf{x})=-\mathbf{x}^2/2$.

The strategy to use should be, by now, clear. First we have to linearize (4.2) around the Ivantsov parabolic solution corresponding to $\sigma=0$. Then we must find the acceptable null eigenvector of $\mathcal{L}^\dagger$, where $\mathcal{L}$ is the linear operator acting on $\zeta_1(r)$. Once the null eigenvector is obtained we can immediately write down the usual solvability condition and derive from it the acceptable values of $\sigma$. Because of the new integral term appearing in Eq. (4.2), this program is more difficult to implement than in the symmetric case.[28] However, we will show that the selected value $\sigma^*(\mu)$ is simply related to that found in the symmetric case

$$\sigma^*(\mu)\simeq\frac{2}{1+\mu}\sigma^*(\mu=1)\ . \quad (4.3)$$

Note that Eq. (4.3) is obviously true if we neglect completely the first integral term in (4.2). In the following we try to explain why this approximation is legal; the reader not particularly interested in the technical details can safely stop at this point.

Let us check explicitly what is the effect of the new term present in (4.2) after the linearization has been performed. The first effect is a modification of the inhomogeneous term in (3.14). We now have the following extra term:

$$g(r)=\int_0^\infty\frac{dr'}{4\pi}r'\mathcal{K}_{iv}H_1(r,r')\ , \quad (4.4)$$

where

$$H_1(r,r')=\tfrac{1}{2}\int_0^{2\pi}d\phi\frac{r^2+r'^2-2rr'\cos\phi}{[r^2+r'^2-2rr'\cos\phi+\frac{1}{4}(r^2-r'^2)^2]^{3/2}}\ , \quad (4.5)$$

and $\mathcal{K}_{iv}$ is given by (3.10). The second, most important difference lies in the resulting form of the operator $\mathcal{L}$, as we can see by looking at the linearized version of (4.2) which should be compared with the $p\to0$ limit of (3.14),

$$\frac{\sigma(1+\mu)}{2r}\frac{d}{dr}(rfA\zeta_1')+\int_0^\infty\frac{dr'}{4\pi}r'H_2(r,r')[\zeta_1(r)-\zeta_1(r')]+\sigma(1-\mu)\int_0^\infty\frac{dr'}{4\pi}H_1(r,r')\frac{d}{dr'}(r'fA\zeta_1')$$
$$+\sigma(1-\mu)\int_0^\infty\frac{dr'}{4\pi}r'\mathcal{K}_{iv}\left[H_3(r,r')[\zeta_1(r)-\zeta_1(r')]+\int_0^{2\pi}d\phi\frac{\zeta_1(r)-\zeta_1(r')+r'\zeta_1'(r')-r\zeta_1'(r')\cos\phi}{[r^2+r'^2-2rr'\cos\phi+\frac{1}{4}(r^2-r'^2)^2]^{3/2}}\right]$$
$$=\frac{\sigma}{2}(1+\mu)\mathcal{K}_{iv}+\sigma(1-\mu)g(r)\ , \quad (4.6)$$

where

$$H_2(r,r')=\int_0^{2\pi}d\phi\frac{r'^2-r^2}{[r^2+r'^2-2rr'\cos\phi+\frac{1}{4}(r^2-r'^2)^2]^{3/2}}\ , \quad (4.7)$$

$H_1(r,r')$ is given by (4.5), and

$$H_3(r,r')=\tfrac{3}{4}(r'^2-r^2)\int_0^{2\pi}d\phi\frac{r^2+r'^2-2rr'\cos\phi}{[r^2+r'^2-2rr'\cos\phi+\frac{1}{4}(r^2-r'^2)^2]^{5/2}}\ . \quad (4.8)$$

The question is now the following. Suppose that, by using (4.6), we write down the equation for the null eigenvector of the adjoint operator and make the familiar WKB ansatz for the form of the solution. How are the terms $S_0$ and $S_1$ in (2.16), which alone determine the asymptotic form of $\sigma^*$, modified by the presence of the extra terms in (4.6)? To answer this question one should note that, although new terms containing high derivatives of $\zeta_1$ appear in (4.6), these terms are multiplied by $\sigma$ and, furthermore, they are inside an integral which acts as a smoothing operator provided the kernel is regular enough. Roughly speaking, the same way as a derivative can be thought to correspond to an effective power of $1/\sqrt{\sigma}$, an integral operator with a regular kernel gives at least one power of $\sqrt{\sigma}$.

To be more precise, consider one of the extra terms appearing in (4.6). We have

$$\sigma(1-\mu)\int_0^\infty\frac{dr'}{4\pi}H_1(r,r')\frac{d}{dr'}(r'fA\zeta_1')=-\sigma(1-\mu)\mathcal{P}\int_0^\infty\frac{dr'}{4\pi}(r'fA\zeta_1')\frac{d}{dr'}H_1(r,r')\ ,$$

where the principal part integral is needed because of the behavior of $H_1(r,r')$ at $r'\simeq r$,

$$H_1(r,r')\simeq -\frac{1}{2r}\ln|r-r'|, \quad r'\simeq r \ .$$

It should be now reasonably clear that the contribution of such a term to the local equation determining $\tilde{Z}(r)$ will be of the form $\sigma\tilde{Z}'(r)$, and hence it will only affect the $r$-dependent prefactor but not the phase function $S_0(r)$.

In an analogous way we can rewrite another term in (4.6) as

$$\sigma(1-\mu)\int_0^\infty \frac{dr'}{4\pi}r'\mathcal{H}_{iv}\int_0^{2\pi}d\phi\frac{\zeta_1(r)-\zeta_1(r')+r'\zeta_1'(r')-r\zeta_1'(r')\cos\phi}{[r^2+r'^2-2rr'\cos\phi+\frac{1}{4}(r^2-r'^2)^2]^{3/2}}$$

$$=\sigma(1-\mu)\int_0^\infty \frac{dr'}{4\pi}r'\mathcal{H}_{iv}\left[H_4(r,r')\frac{d}{dr'}\left[\frac{\zeta_1(r')-\zeta_1(r)}{r'-r}\right]+r\zeta_1'(r')H_5(r,r')\right],$$

where

$$H_4(r,r')=\int_0^{2\pi}d\phi\frac{(r'-r)^2}{[r^2+r'^2-2rr'\cos\phi+\frac{1}{4}(r^2-r'^2)^2]^{3/2}} \tag{4.9}$$

and

$$H_5(r,r')=\int_0^{2\pi}d\phi\frac{1-\cos\phi}{[r^2+r'^2-2rr'\cos\phi+\frac{1}{4}(r^2-r'^2)^2]^{3/2}} \ . \tag{4.10}$$

An analysis of the local behavior of $H_4(r,r')$ and $H_5(r,r')$ at $r'\simeq r$ shows that we can integrate such a term by parts and that its contribution to the $\tilde{Z}(r)$ equation, being of the form $\sigma\tilde{Z}$, can be neglected altogether. The same is true for the remaining term in (4.6).

The net result is that the extra terms present in (4.6) can be neglected in determining the phase function $S_0(r)$. A more careful analysis shows that the result for $\tilde{Z}(r,\mu,\sigma)$ is of the form

$$\tilde{Z}(r,\mu,\sigma)=\exp\left[-\frac{i}{8}\frac{1-\mu}{1+\mu}r\right]\tilde{Z}(r,\sigma(\mu)) \ , \tag{4.11}$$

where $\tilde{Z}(r,\sigma(\mu))$ is the solution in the symmetric limit with $\sigma$ replaced by $\sigma(1+\mu)/2$ and $p=0$.

We can now consider the solvability condition analogous to Eq. (3.15),

$$\Lambda_3(\sigma,\alpha,\mu)=\mathrm{Re}\int_0^\infty dr\frac{\sqrt{r}\,(1+r^2)^{3/4}}{\sqrt{A}}\left[\frac{1+\mu}{2}\mathcal{H}_{iv}+(1-\mu)g(r)\right]\tilde{Z}(r,\mu,\sigma)e^{-i(\pi/4)}=0 \ . \tag{4.12}$$

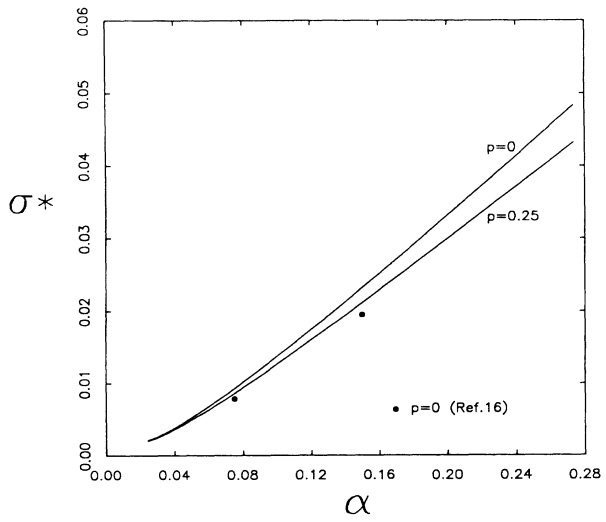


FIG. 2. Selected values $\sigma^*$ as a function of the anisotropy strength $\alpha$ for $p=0$ and $p=0.25$ in three dimensions. Comparison with a direct numerical integration of Eq. (3.6).

In the case $\alpha\ll 1, \sigma\ll 1$, we know that II is dominated by the behavior of the integrand in a neighborhood of $r=i$. For this reason, in this limit we can replace $\tilde{Z}(r,\mu,\sigma)$ by $\tilde{Z}(r,\sigma(\mu))$. Furthermore one can check that the contributions to $\Lambda_3(\sigma,\alpha,\mu)$ coming from the two terms in the square brackets under the integral sign scale in a different way with $\sigma$, as $\sigma\to 0$ and $\alpha\ll 1$, and the dominant one comes from the $\mathcal{H}_{iv}$ term. The result of all this is simply that (4.3) indeed represents the correct asymptotic form of $\sigma^*(\mu)$.

## ACKNOWLEDGMENTS

This research was supported by U.S. Department of Energy Grant No. DE-FG03-84ER45108 and by National Science Foundation Grant No. PHY-82-17853, supplemented by funds from the U.S. National Aeronautics and Space Administration.

## APPENDIX A

In this appendix we give a detailed derivation of (2.18). We will assume that the analytic continuation for complex $x$ of the phase function $S_0(x)$ defined in (2.16) and

(2.17) has a vanishing derivative at some point $x=\bar{x}$ in the upper half plane. This means that $x=\bar{x}$ is a point of stationary phase for the rapidly varying function $\tilde{Z}(x)$, and hence the integrals appearing in (2.15) can be estimated, in the limit $\sigma\to 0$, by a steepest descent approximation. To do this we deform the contour of integration in the upper plane so that it goes through $x'=\bar{x}$, and then we extract the leading contributions.

In order to deform the contour we need to consider the singularities of the kernel $I(x',x)$ on the real $x'$ axis; it is easily checked that the only singularity occurs at $x'=x$ and, by using the limiting form of the Bessel functions at small argument,[19] we obtain the following expression for $I(x',x)$ in a neighborhood of the singular point:

$$I(x',x)=\frac{x(1+x^2)^{1/2}}{pA(x-x')}-\frac{(1+x^2)^{3/2}}{2A}\ln(x-x')^2+\cdots \qquad (x'\to x)\ . \tag{A1}$$

We see that the function $I(x',x)$ has both a pole and a branch cut at $x=x'$. If we now assume, and this will serve as a self-consistency check at the end of the calculation, that $\mathrm{Re}S_0(\bar{x})<0$, the dominant contributions to the integral appearing in (2.15) will only come from the integration in a neighborhood of $x'=x$. After a proper analytic continuation of $I(x',x)$ in a complex neighborhood of such a point and by using (A1) and (2.15)–(2.17), we finally obtain the following local equation, correct to order $\sqrt{\sigma}$:

$$\sigma\exp\left[-\frac{S(x,\sigma)}{\sqrt{\sigma}}\right]\frac{d^2}{dx^2}\exp\left[\frac{S(x,\sigma)}{\sqrt{\sigma}}\right]$$

$$-i\sqrt{\sigma}\frac{p(1+x^2)^{3/2}}{A(x)S'(x)}+\frac{(1+x^2)^{1/2}}{A(x)}(1+ix)=0\ . \tag{A2}$$

To obtain $S_0$ and $S_1$, and hence (2.18), we simply need to evaluate the second derivative and to expand the resulting equation in powers of $\sqrt{\sigma}$ by using (2.17). Note that of the two possible choices for $S_0(x)$, we must take the one satisfying the condition $\mathrm{Re}S_0(\bar{x})<0$. Once we have the desired solution $\tilde{Z}(x)$, it is evident from Eq. (2.15) that another acceptable solution will be given by $\tilde{Z}^*(x)$.

## APPENDIX B

In this appendix we give some of the details of the three-dimensional calculation reported in Sec. III. The derivation of Eq. (3.10) is very simple. First notice that, upon linearization, the term in square brackets on the left-hand side of Eq. (3.6) can be written as

$$\mathcal{K}_{iv}-Af\xi_1''-\xi_1'\left[Af'+A'f+\frac{Af}{r}\right]-\xi_1'\left[\frac{Bf}{r}-\frac{Af}{r}+\frac{B'}{(1+r^2)^{1/2}}\right],$$

where

$$\mathcal{K}_{iv}=\frac{A(r)}{(1+r^2)^{3/2}}+\frac{B(r)}{(1+r^2)^{1/2}}\ , \tag{B1}$$

$$f(r)=\frac{1}{(1+r^2)^{3/2}}\ , \tag{B2}$$

with $A(r)$ and $B(r)$ obtained from (3.5) and (3.8) by setting $\tan\theta=r$,

$$A(r)=1-\frac{4\alpha}{5}+\frac{\alpha}{15}\frac{34r^2-1}{(1+r^2)^2}\ , \tag{B3}$$

$$B(r)=1-\frac{\alpha}{5}\frac{5-2r^2}{(1+r^2)^2}\ . \tag{B4}$$

Equation (3.10) is now a consequence of the equality

$$\frac{Bf}{r}-\frac{Af}{r}+\frac{B'}{(1+r^2)^{1/2}}=0\ ,$$

which holds independently of the choice of $\gamma(\bar{\theta})$. This can be seen most easily if we go back to the $\theta$ variable $\tan\theta=r$, rewrite the equation as

$$[B(\theta)-A(\theta)]\frac{\cos^3\theta}{\tan\theta}+\cos\theta\left[\frac{d\tan\theta}{d\theta}\right]^{-1}\frac{dB}{d\theta}=0\ ,$$

and use the expression for $A$ and $B$ as given by (3.8).

Finally we analyze (3.13) to derive (3.14). Notice that there are two main differences between the two- and three-dimensional cases. The first is that the integral in (3.13) is for $r'\geq 0$ only; the second is that the integral kernel $H(r,r')$ cannot be explicitly defined in terms of elementary functions. As we shall see these two facts complicate the algebraic part of the analysis without, however, changing the essence of the two-dimensional derivation.

Proceedings as in two dimensions we have now to deform the contour of integration in the appropriate way. In addition to the pole and the branch cut contributions, there is also a term coming from the integration along part of the imaginary axis (see Fig. 3). Actually this last term does not give any contribution when we consider the acceptable solution defined in (3.14), we will come back to this point later on, and hence we can keep just the local contribution from the singular point as we did in 2$d$. This can be obtained by computing the behavior of $H(r',r)$ in a neighborhood of $r'=r$,

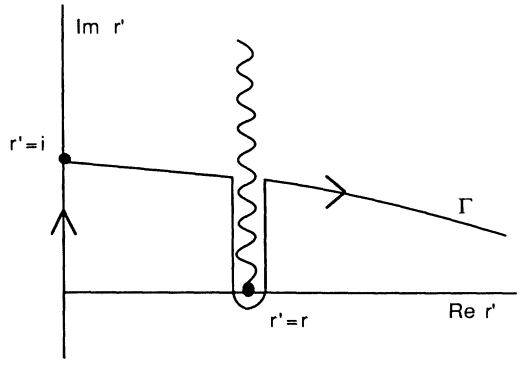


FIG. 3. Contour of integration used to simplify Eq. (3.13).

$$H(r',r)=\frac{r(1+r^2)^{1/2}}{A(r)(r-r')} - \frac{(1+r^2)^{3/2}}{2A}\ln(r-r')^2+\cdots \quad (r'\to r) . \quad \text{(B5)}$$

The local behavior of the integral kernel is identical to what we found in the two-dimensional case so that we can write down at once the equation replacing (3.13) in the limit $\sigma\to 0$. By comparing (3.13) and (2.15) we obtain

$$\sigma\exp\left[-\frac{S(r,\sigma)}{\sqrt{\sigma}}\right]\frac{d^2}{dr^2}\exp\left[\frac{S(r,\sigma)}{\sqrt{\sigma}}\right]+\frac{\sigma}{4r^2} -i\sqrt{\sigma}\frac{p(1+r^2)^{3/2}}{A(r)S'(r)}+\frac{(1+r^2)^{1/2}}{A(r)}(1+ir)=0 . \quad \text{(B6)}$$

Also in this case, of course, the solution of (B6) has to be chosen so to satisfy the self-consistency requirement $\mathrm{Re}S_0(\bar{r})<0$ at the point of stationary phase $r=\bar{r}$ in the upper half plane.

Equation (B6) is almost identical to (A2); indeed, if $r\gg\sqrt{\sigma}$, the solution is immediately given by (2.18) provided we use (B3) for $A(r)$. The two solution $\tilde{Z}(r)$ and $\tilde{Z}^*(r)$ must now be combined in a way to satisfy the boundary condition at $r=0$. In order to do so we can solve (B6) for $r\ll 1$ and use asymptotic matching[29] to obtain a global solution for $r\geq 0$.

If $r\ll 1$, by taking into account the boundary condition at $r=0$ we can reduce (B6) to

$$\sigma\tilde{Z}''(r)+\left[\frac{\sigma}{4r^2}+\frac{1}{1-\frac{13}{15}\alpha}\right]\tilde{Z}(r)=0 , \quad \text{(B7)}$$

whose solutions are given by

$$\tilde{Z}_1(r)=\sqrt{r}J_0\left[\frac{r}{\sqrt{\sigma(1-\frac{13}{15}\alpha)}}\right] ,$$

$$\tilde{Z}_2(r)=\sqrt{r}Y_0\left[\frac{r}{\sqrt{\sigma(1-\frac{13}{15}\alpha)}}\right] ,$$

where $J_0$ and $Y_0$ are Bessel functions of order zero. The boundary condition to impose at $r=0$ requires that we choose the linear combination of $\tilde{Z}(r)$ and $\tilde{Z}^*(r)$ which is proportional to $\tilde{Z}_1(r)$ as $r\ll 1$. This combination can be obtained if we notice that the solutions of (B6) and (B7) must agree in the region $\sqrt{\sigma}\ll r\ll 1$, where both equations are valid. For these values of $r$ we can approximate $J_0$ by using its asymptotic expansion for large argument, which can then be compared with the expression of $\tilde{Z}(r)$ and $\tilde{Z}^*(r)$ in the limit $r\ll 1$. In this way it is easy to check that the appropriate combination giving the correct boundary condition at $r=0$ is indeed given by (3.14).

Finally, we can verify that neglecting the integral along the imaginary axis to obtain (B6) was legal. We substitute (3.14) in (3.13) and proceed in evaluating the integral by steepest descent. [Note that the contour has to be deformed into the lower plane when integrating $\tilde{Z}^*(r)$.] We see that the two terms

$$\int_0^i\tilde{Z}(r')H(r',r)dr'/\pi$$

and

$$\int_0^{-1}\tilde{Z}^*(r')H(r',r)dr'/\pi$$

exactly cancel each other. This is a consequence of the identities

$$H(e^{-i(\pi/2)}x,r')=e^{-i(\pi/2)}H(e^{i(\pi/2)}x,r') ,$$

$$\tilde{Z}^*(e^{-i(\pi/2)}x)=\tilde{Z}(e^{i(\pi/2)}x) ,$$

which are valid for real $x$ and can be checked by using (3.12) and (2.18) and (2.19).

*Present address: Department of Physics, University of California, Santa Cruz, Santa Cruz, CA 95064.

[1]As a general review about recent theoretical developments the reader is referred to J. S. Langer, in *Chance and Matter,* 1986 Les Houches Lectures XLVI (Elsevier, New York, 1987); D. A. Kessler, J. Koplik, and H. Levine, Adv. Phys. **37**, 255 (1988).

[2]G. P. Ivantsov, Dokl. Akad. Nauk. SSSR **58**, 567, (1947).

[3]D. A. Kessler and H. Levine, Phys. Rev. Lett. **57**, 3069 (1986).

[4]M. E. Glicksman, R. J. Shaefer, and J. D. Ayers, Metall. Trans. A **7**, 414 1976.

[5]S. C. Huang and M. E. Glicksman, Acta Metall. **29**, 701 (1981); **29**, 717 (1981).

[6]A. Dougherty, P. D. Kaplan, and J. P. Gollub, Phys. Rev. Lett. **58**, 1652 (1987).

[7]A. Dougherty and J. P. Gollub, Phys. Rev. A **38**, 3043 (1988).

[8]P. Pelcé and Y. Pomeau, Stud. Appl. Math. **74**, 245 (1986).

[9]B. Caroli, C. Caroli, B. Roulet, and J. S. Langer, Phys. Rev. A **33**, 442 (1986).

[10]M. Ben-Amar and Y. Pomeau, Europhys. Lett. **2**, 307 (1986); Phisicochem. Hydrodyn. (to be published).

[11]A. Barbieri, D. Hong, and J. S. Langer, Phys. Rev. A **35**, 1802 (1987).

[12]D. A. Kessler, J. Koplik, and H. Levine, Phys. Rev. A **33**, 3352 (1986).

[13]D. Meiron, Phys. Rev. A **33**, 2704 (1986).

[14]Y. Saito, G. Goldbeck-Wood, and H. Müller-Krumbhaar, Phys. Rev. Lett. **58**, 1541 (1987).

[15]M. Ben-Amar and B. Moussallam, Physica D **25**, 155 (1987).

[16]D. A. Kessler and H. Levine, Phys. Rev. A **36**, 4123 (1987).

[17]R. Combescot, T. Dombre, V. Hakim, Y. Pomeau, and A. Pumir, Phys. Rev. Lett. **56**, 2036 (1986); Phys. Rev. A **37**, 1270 (1988).

[18]See J. S. Langer, Rev. Mod. Phys. **1**, 52 (1980) for the correct interpretation of the parameters and fields in this case.

[19]*Handbook of Mathematical Functions,* edited by M. Abramowitz and I. A. Stegun (Dover, New York, 1972).

[20]B. Caroli, C. Caroli, C. Misbah, and B. Roulet, J. Phys. (Paris) (to be published).

[21]This fact is not such a suprise, especially in view of some re-

cent analytic work on the mathematically related problem of the Saffman-Taylor finger; see R. Combescot, T. Dombre, V. Hakim, Y. Pomeau, and A. Pumir, Phys. Rev. A **37**, 1270 (1988). What is probably true also in the case we are considering is that, although the linearization fails to predict the overall amplitude of the cusp at the tip (which is simply related to the solvability function $\Lambda$) in the case in which the solvability condition is not satisfied, the same method gives, nevertheless, the right answer for those values of $\sigma$, determined by the solvability condition (1.1), which make the amplitude of $\Lambda$ irrelevant.

[22]A. Barbieri, Ph.D. thesis, University of California at Santa Barbara, 1988.

[23]B. I. Shraiman, Phys. Rev. Lett. **56**, 2028 (1986).

[24]Indeed, even for $\alpha=0.5$ comparison with Ref. 15 shows that the relative error in the case $p=0$ is equal to 12%.

[25]D. P. Woodruff, *The Solid-Liquid Interface* (Cambridge University Press, London, 1973).

[26]D. A. Kessler and H. Levine (unpublished).

[27]In the one-sided limit $\mu=0$, this generalization is almost straightforward because the system (4.1) decouples and it is easy to derive a single equation involving only the function $\zeta(\mathbf{x})$.

[28]C. Misbah, J. Phys. (Paris) **48**, 1265 (1987).

[29]C. M. Bender and S. A. Orszag, *Advanced Mathematical Methods for Scientists and Engineers* (McGraw-Hill, New York, 1978).